Carcinogenesis vol.26 no.11 pp.1999–2009, 2005
doi:10.1093/carcin/bgi150
Advance Access publication June 13, 2005

Life-span inhalation exposure to mainstream cigarette smoke induces lung cancer in B6C3F1 mice through genetic and epigenetic pathways

Julie A.Hutt*, Brian R.Vuillemenot, Edward B.Barr, Marcie J.Grimes, Fletcher F.Hahn, Charles H.Hobbs, Thomas H.March, Andrew P.Gigliotti, Steven K.Seilkop[1], Gregory L.Finch[2], Joe L.Mauderly and Steven A.Belinsky

Lovelace Respiratory Research Institute, 2425 Ridgecrest Drive SE, Albuquerque, NM 87108, USA, [1]SKS Consulting Services, Siler City, 3942 Rives Chapel Church Road, Siler City, NC 27344, USA and [2]Pfizer Global Research and Development, Groton Laboratories, Mount Eastern Point Road, Groton, CT 06340, USA

*To whom correspondence should be addressed. Tel: +1 505 348 9567; Fax: +1 505 348 8567;
Email: jhutt@lrri.org

Although cigarette smoke has been epidemiologically associated with lung cancer in humans for many years, animal models of cigarette smoke-induced lung cancer have been lacking. This study demonstrated that life time whole body exposures of female B6C3F1 mice to mainstream cigarette smoke at 250 mg total particulate matter/m^3 for 6 h per day, 5 days a week induces marked increases in the incidence of focal alveolar hyperplasias, pulmonary adenomas, papillomas and adenocarcinomas. Cigarette smoke-exposed mice ($n = 330$) had a 10-fold increase in the incidence of hyperplastic lesions, and a 4.6-fold (adenomas and papillomas), 7.25-fold (adenocarcinomas) and 5-fold (metastatic pulmonary adenocarcinomas) increase in primary lung neoplasms compared with sham-exposed mice ($n = 326$). Activating point mutations in codon 12 of the *K-ras* gene were identified at a similar rate in tumors from sham-exposed mice (47%) and cigarette smoke-exposed mice (60%). The percentages of transversion and transition mutations were similar in both the groups. Hypermethylation of the *death associated protein (DAP)-kinase* and *retinoic acid receptor (RAR)*-β gene promoters was detected in tumors from both sham- and cigarette smoke-exposed mice, with a tendency towards increased frequency of *RAR*-β methylation in the tumors from the cigarette smoke-exposed mice. These results emphasize the importance of the activation of *K-ras* and silencing of *DAP-kinase* and *RAR*-β in lung cancer development, and confirm the relevance of this mouse model for studying lung tumorigenesis.

Introduction

Lung cancer is currently the leading cause of cancer death in the United States, with a 5 year survival rate of 15% (1). The high mortality is in part due to the poor response to therapy at the advanced stage in which the disease is typically diagnosed. Approximately 90% of all lung cancers are attributed to cigarette smoking. Lung cancer in humans is histopathologically categorized as small cell or non-small cell lung cancer, with the non-small cell category including squamous cell carcinoma, large cell carcinoma and adenocarcinoma. In recent years, the incidence of pulmonary adenocarcinoma has increased, particularly in women, and it is now the most common histological type of lung cancer (2,3). The development of lung adenocarcinoma now appears to be strongly linked with cigarette smoking, with changes in the smoking behavior and cigarette design thought to contribute to the increased incidence of adenocarcinoma.

Until recently, attempts at inducing lung cancer in animals using cigarette smoke (CS) have not been very successful. Increases in the incidence of lung tumor formation have been reported in A/J and SWR mice exposed to environmental or mainstream CS for 5 months, followed by recovery in air for 4 months (4–7). However, in two of these studies, CS exposure resulted in a significant decrease in malignant lung tumors compared with controls (4,5). In addition, exposure of A/J mice to mainstream CS for 6 h/day, 5 days a week for 26 weeks followed by recovery in air for 5 weeks did not increase lung tumor formation or promote nitrosamine-4-(methylnitrosamino)-1-(3-pyridyl)-1-butanone (NNK)-induced tumors (8). Until the recent report by Mauderly *et al*. (9) describing CS-induced lung and nasal tumors in rats, chronic CS inhalation studies in other rodents, dogs and non-human primates have generally not produced statistically significant increases in lung tumor formation (10–12).

In spontaneous and chemically-induced murine lung tumors, many of the signaling pathways that are disrupted through genetic and epigenetic alterations in oncogenes and tumor suppressor genes are identical to those that are disrupted in human lung cancer (13–16). Thus, a mouse model of CS-induced lung carcinogenesis would be a valuable tool for conducting research on the molecular mechanisms of CS-induced lung cancer.

The mutation profile of the *K-ras* oncogene is well documented in lung cancer. Activating point mutations in the *K-ras* gene arise through promutagenic DNA adduct formation in response to carcinogen exposure. *K-ras* is mutated in ~20–56% of human lung cancers, with most mutations occurring in adenocarcinomas (17–22). *K-ras* mutations in human lung adenocarcinomas occur primarily at codon 12 (GGT→GAT, and GGT→GTT) and, until recently, were described more commonly in adenocarcinomas from smokers and former smokers than from never-smokers (18,19,21,22). However, a recent study found the incidence of codon 12 *K-ras* mutations in smokers and never-smokers to be similar, with a preponderance of transversion mutations occurring in both the groups (20). Codon 12 transition mutations (66%) and transversion mutations (34%) have also been reported in ~17% of spontaneous lung tumors from control B6C3F1 mice used in the

Abbreviations: CS, cigarette smoke; DAP-kinase, death associated protein kinase; RAR-β, retinoic acid receptor-β; NNK, nitrosamine-4-(methylnitrosamino)-1-(3-pyridyl)-1-butanone; NTP, National Toxicology Program; B[*a*]P, benzo[*a*]pyrene; TPM, total particulate matter; NBF, neutral buffered formalin; MSP, methylation-specific PCR.

National Toxicology Program (NTP) bioassay (23). In chemically-induced lung tumors from A/J mice, the tobacco-specific nitrosamine NNK, and the polyaromatic hydrocarbon benzo[*a*]pyrene (B[*a*]P) are the CS carcinogens that have been associated with the formation of transition and transversion mutations in the *K-ras* gene, respectively (24–26).

Inactivation of genes by promoter methylation has emerged as a critical component of lung cancer development and progression (27). Two genes commonly inactivated in human lung cancer, *death associated protein (DAP)-kinase* and *retinoic acid receptor-beta* (*RAR*-B), are also inactivated in murine cancer development. The *DAP-kinase* gene is a serine-threonine protein kinase with a role in apoptosis induction. Inactivation of *DAP-kinase* by promoter hypermethylation occurs in many human tumor types, including 23–44% of non-small cell lung cancers (28–30). Transcriptional silencing of the *DAP-kinase* gene by hypermethylation has previously been reported in 52% of mouse lung tumors induced by the tobacco-specific nitrosamine NNK, along with 60 and 50% of mouse lung tumors induced by vinyl carbamate and methylene chloride, respectively (15). Furthermore, the rate of *DAP-kinase* inactivation was similar in NNK-induced hyperplastic foci and adenocarcinomas indicating that *DAP-kinase* inactivation is an early event in murine lung carcinogenesis (15).

Retinoids regulate cell differentiation and growth through binding to members of the retinoic acid receptor family. The ligand bound heterodimeric receptors then bind to DNA and function as transcription factors. *RAR*-β has anti-tumor properties that are mediated through inhibition of proliferation and metastases, and induction of apoptosis (31,32). Loss of *RAR*-β expression occurs in 41% of all human non-small cell lung cancers via promoter hypermethylation (33). Recently, loss of *RAR*-β expression through hypermethylation was shown in 85, 56 and 60% of murine lung tumors induced by NNK, methylene chloride and vinyl carbamate, respectively (14). A small number of tumors induced by the CS exposure described below were also examined for methylation of the *DAP-kinase* and *RAR*-β genes (14,15). Methylation of *DAP-kinase* and *RAR*-β were detected in 43 and 90% of these tumors, respectively.

This paper investigates the utility of the CS-exposed B6C3F1 mouse as a model for CS-induced lung cancer. B6C3F1 mice were used in this investigation due to their low background incidence of lung cancer and their use in the NTP bioassay program. In order to better understand the mechanisms for tumor development in this model, the mutation profile for the *K-ras* gene and methylation of the *DAP-kinase* and *RAR*-β genes were compared in an expanded sample set of CS-induced lung tumors versus spontaneously arising lung tumors.

Materials and methods

Animals

Female B6C3F1 mice were used in this study. These mice were exposed to CS as part of a larger experiment examining the combined effects of CS and $^{239}PuO_2$, and CS and thoracic X-rays. Only female mice were used in this study in order to increase the statistical power of the analysis. Specific pathogen free mice (Charles River Laboratories, Raleigh, NC) were received at 4–6 weeks of age. Mice were quarantined and conditioned to exposure chambers for 2 weeks, weighed and randomized by weight for assignment to treatment groups. Mice were housed individually and provided water *ad libitum* via an automated watering system. Food (Wayne Lab Blox, Allied Mills, Chicago, IL) was provided *ad libitum* except during exposures, in order to decrease the gastrointestinal intake of smoke particles. Chamber temperatures were maintained at 20–24°C with 40–70% relative humidity. Standard fluorescent lights were maintained on a 12 h light/dark cycle. Animals were observed twice a day and moribund animals were euthanized. Mice were weighed periodically throughout the study. Sera from sentinel animals were collected during the exposure period and confirmed to be negative for the antibodies to the following common murine pathogens: Epizootic Diarrhea of Infant Mice, Theiler's Mouse Encephalomyelitis Virus, Mouse Hepatitis Virus, Mice Minute Virus, Mouse Parvovirus, Sendai Virus, Pneumonia Virus of Mice, Lymphocytic Choriomeningitis Virus, *Mycoplasma pulmonis* and Cilia Associated Respiratory Bacillus (Mouse Intermediate Antibody Profile, Microbiological Associates, Rockville, MD).

Cigarette smoke exposure

All animal exposure protocols were approved by the Institutional Animal Care and Use Committee. Mice were exposed in whole body inhalation exposure chambers (Hazelton H2000, Lab Products, Maywood, NJ) to mainstream CS diluted to 250 mg total particulate matter (TPM)/m^3 (330 mice) or to HEPA-filtered air (326 mice, as controls) for 6 h/day, 5 days a week for 30 months, starting at 6 weeks of age. This large number of mice was used in order to increase the statistical power of the analysis, as a low level of tumor induction was anticipated, and to provide adequate amounts of tissue samples for multiple investigators. This exposure level was selected because previous studies in F344 rats showed that it was sufficient to induce lung tumors without a significant increase in mortality (9). CS was generated from unfiltered 2R1 research cigarettes (Tobacco Health Research Institute, Lexington, KY) that were stored in a freezer and conditioned overnight before use at 24°C and 50–70% relative humidity. Using a modified commercial smoke generator (AMESA, Type 1300, Geneva, SW) the cigarettes were puffed twice per minute using a 70 ml 2 s puff.

Exposure concentrations were determined gravimetrically from filter samples taken three times a day from the mid-point of each chamber. Particle size distribution was measured periodically using a multi-jet Mercer cascade impactor (34). The dosimetry of carbon monoxide in CS was estimated by measuring the blood carboxyhemoglobin levels in nine CS-exposed and nine sham-exposed mice 32 weeks after the initiation of smoke exposures. Chambers were purged for 20 min after the daily smoke exposure, animals were removed and anesthetized, and cardiac blood was withdrawn into heparinized syringes. Samples were placed on ice and carboxyhemoglobin was assayed spectrophotometrically (IL-282 Co-oximeter, Instrumentation Laboratory, Lexington, MA). Previous reports describe the smoke composition in greater detail (35,36).

Necropsy and histology

Mice were euthanized in a moribund state or were killed at the study termination by an overdose of intraperitoneal sodium pentobarbital and exsanguination. A complete necropsy was performed on all mice and all the gross lesions were recorded. Lungs were removed from the thorax *en bloc*, weighed and inflated with 4% paraformaldehyde via a tracheal cannula. Lungs and gross lesions were fixed for 24–72 h in 4% paraformaldehyde and subsequently trimmed for paraffin embedding. Lungs were trimmed along the major axial airways of the left lung and the right cranial, middle and caudal lobes. Gross lung lesions and gross lesions in other tissues were also sectioned. Nasal cavities were flushed with 10% neutral buffered formalin (NBF) through the nasopharynx and fixed by submersion in NBF, followed by decalcification in 13% formic acid. Decalcified nasal cavities were sectioned transversely at three levels (immediately caudal to the upper incisors, immediately caudal to the incisive papilla and at the middle of the upper second molar) to allow for microscopic examination of the nasal vestibule and multiple areas lined by respiratory, transitional and olfactory mucosa. Paraffin-embedded tissues were sectioned at 5 μm and stained with hematoxylin and eosin for the histological analysis.

Histopathologic evaluation

Lung and nasal cavity sections were first examined by a single board-certified veterinary pathologist. Histological evaluations of the lung and nasal sections were focused on proliferative lesions. Additional tissues from gross lesions were examined as required to exclude pulmonary metastases from the non-pulmonary tissues, and to identify metastases from primary lung or nasal tumors. Lung tumors were then reviewed by three additional board-certified veterinary pathologists and consensus diagnoses were developed. Primary lung tumors were classified according to the guidelines recently established by the Mouse Models of Human Cancers Consortium (37). Accordingly, use of the term bronchioloalveolar was withheld in order to avoid confusion with the specific subtype of human adenocarcinoma known as bronchioloalveolar adenocarcinoma.

Cell culture

Cell lines and A/J lung tumors induced by NNK exposure (CL25 and CL30) were used as positive controls for the methylation assays (14,15,26). These cell lines were isolated from tumors collected at necropsy and their malignant potential was verified by injection into the subcutaneous tissues of nude mice (data not shown). The cell lines were grown in RPMI or ITRI-1 media at 37°C in a humid atmosphere containing 5% CO_2 (38). DNA was isolated from the cells by digestion with 1% pronase and phenol–chloroform extraction.

Analysis of codon 12 K-ras mutations

Tumors from cell lines and from sham-exposed and CS-exposed mice were examined for mutations in codon 12 of the *K-ras* gene. Adenomas and adenocarcinomas >2 mm in diameter were microdissected from paraffin sections, followed by tissue digestion with 1% pronase and phenol–chloroform extraction of DNA. Codon 12 mutations were assessed using the *Bst*N1 (New England BioLabs, Beverly, MA) restriction fragment length polymorphism technique (39). Briefly, a 142 bp fragment containing *K-ras* exon 1 was amplified using primers flanking the ends of exon 1. An aliquot of the first stage reaction mixture was then amplified using a second set of inner primers containing a G:C mismatch in the sense strand corresponding to the first nucleotide of codon 11. This mismatch creates a BstN1restriction site (CC[T/A]GG) in wild-type *K-ras* codon 12. The 95 bp product containing wild-type codon 12 digests with BstN1 into 63 and 32 bp fragments, whereas point mutations at either of the first two positions of codon 12 prevent the BstN1 digestion. Frozen, normal B6C3F1 mouse lung served as a negative control. The products were visualized on 3% agarose TBE gels. Codon 12 mutations were verified by isolating the bands that did not digest with BstN1 followed by reamplification and sequencing (Sequetech, Mountain View, CA). A total of 45 tumors from CS-exposed animals and 15 tumors from sham-exposed animals were of sufficient size for the evaluation. Because of the small amounts of tumor tissue available for analyses, not all the tumors analyzed for *K-ras* mutations could also be analyzed for methylation.

Methylation-specific PCR

The methylation status of the murine *RAR*-β and *DAP-kinase* promoters was determined using nested, two-stage methylation-specific polymerase chain reaction (MSP) assay, as described previously (14,15). Frozen lung from two normal B6C3F1 mice served as negative controls and cell lines derived from two NNK-induced tumors that have previously been shown to be methylated served as positive controls. The products were visualized on 3% agarose TBE gels. Adenomas and adenocarcinomas from 37 CS-exposed animals and 15 sham-exposed animals were of sufficient size for the evaluation. Because of the small amounts of tumor tissue available for analyses, not all the tumors analyzed for methylation could also be analyzed for *K-ras* mutations.

Statistical analysis

Statistical significance was tested and reported at multiple levels; however, the minimum criterion for statistical significance was set at $P = 0.05$.

Survival. The product-limit method of Kaplan and Meier (40) was used to obtain survival estimates as a function of weeks on study. Cox's proportional hazards model (41) was used to test equality of survival rates between the CS-exposed and sham control groups. Reported *P*-values are two-sided.

Body and lung weights. Mean body weights for the sham- and CS-exposed mice were compared by unequal variance *t*-test at intervals throughout the study. Terminal body weights and terminal lung weights were compared between sham- and CS-exposed animals with an unequal variance *t*-test with the Satterthwaite adjustment for degrees of freedom (42). The mean and standard error of the mean are reported for each exposure group.

Neoplastic lesions. Neoplasms were assumed to be incidental to death, and were analyzed using logistic regression (43,44). Lesion incidence was modeled as a logistic function of exposure concentration and time. Linear and quadratic temporal terms were used, and the quadratic term was eliminated if it did not significantly enhance the fit of the model. Both pairwise comparisons of smoke-exposed groups with controls and an overall trend test were performed. When the logistic regression failed to converge mathematically, the continuity-corrected incidental tumor test was applied (45). Lesion multiplicities were calculated as the total number of observed lesions divided by the number of lesion-bearing animals; comparisons between control and CS-exposed animals were performed using weighted least squares analysis of variance for categorical data (46). Reported *P*-values are two-sided.

Examination of lymphosarcoma/body weight relationship. The relationship between tumor incidence and body weight was examined for lymphosarcomas to determine if decreased lymphosarcoma incidence in smoke-exposed mice could be attributed to lower body weight corresponding to smoke exposure. Relationships between tumor incidence and body weight in mice have been found for several tumor types, and methods have been developed to perform a statistical analysis that accounts for weight differences in treated and control animals (47). Following this approach, lymphosarcoma incidence was modeled as a logistic function of terminal body weight, day of death, exposure (sham versus smoke) and the interaction between exposure and body weight. The significance of the relationship between lymphosarcoma incidence and body weight was assessed using the logistic regression-based Wald test and the composite test of non-null logistic regression terms for exposure, and the interaction between exposure and body weight was used to assess the significance of differences in the relationships between tumor incidence and body weight for smoke-exposed and sham-exposed animals (48).

K-ras mutation/methylation status. The distributions of codon 12 *K-ras* mutation types in sham- and CS-exposed animals were compared with the χ^2-test and Fisher's exact test. Proportions of tumors with *RAR*-β and *DAP-kinase* methylation in sham-exposed and CS-exposed mice were compared with the two-tailed Fisher's exact test. Independence between genes was tested by χ^2 and Fisher's exact tests.

Results

Cigarette smoke exposure

Daily and study average (254 ± 27 mg/m^3, mean ± SD of daily values) smoke TPM levels were maintained close to target levels throughout the 2.5 year exposure period. Concentrations of gases measured at four intervals during the study were elevated (CO = 171 ± 34 p.p.m., NO_x = 2.25 ± 0.48 p.p.m., hydrocarbons = 62 ± 22 p.p.m., mean ± SD). The blood carboxyhemoglobin level for CS-exposed mice after 32 weeks of exposure was determined to be 10.5 % ± 2.9% (mean ± SD) compared with −0.2 ± 0.3% in sham-exposed control mice. The mass median aerodynamic diameters and geometric standard deviations of particle size were 0.59 μm and 1.32 σ_g ($n = 16$), respectively.

Survival

The Kaplan–Meier survival curve is shown in Figure 1. At the end of the study (918–930 days) 19.9% of sham-exposed control mice were alive compared with 47.3% of CS-exposed mice ($P < 0.001$).

Body and lung weights

Mice were weighed at intervals throughout the study. An exposure-related decrease in body weight gain is demonstrated in Figure 2. At all weighing intervals after exposures were started, the mean body weight of CS-exposed mice was significantly less than the mean body weight of sham-exposed mice ($P < 0.001$). Mean (±standard error) terminal body weights

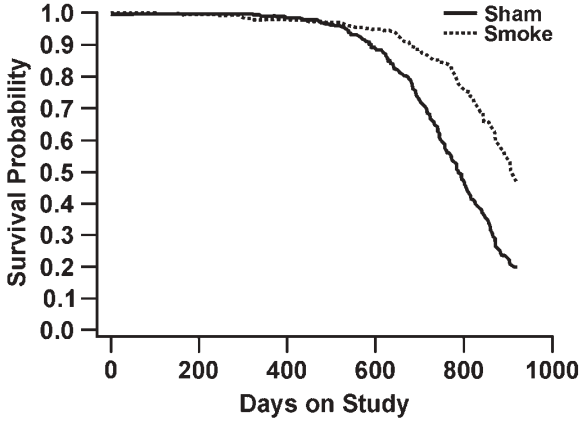

Fig. 1. Kaplan–Meier survival curve. The first terminal sacrifice occurred at 918 days after the initiation of exposures.

for the CS-exposed mice (23.06 ± 0.19 g) were also significantly lower than those for the sham-exposed mice (31.67 ± 0.38 g) ($P < 0.001$). In contrast, mean (± standard error) terminal lung weights from CS-exposed mice (0.619 ± 0.002) were significantly greater ($P < 0.001$) than the mean terminal lung weights from sham-exposed mice (0.398 ± 0.001).

Non-proliferative lung lesions associated with exposure to CS

The most commonly observed lung lesion associated with exposure to CS was increased numbers of alveolar macrophages, many of which were large and binucleated, and had a yellowish-brown granular cytoplasmic pigment. These macrophages were present individually and also as small clusters within the alveoli and were often mixed with variable numbers of neutrophils and cell debris (data not shown). Similar infiltrates were present within the peribronchiolar connective tissues and the adventitia of vessels, often in nodular aggregates with the formation of granulomas surrounded by lymphocytes. Small numbers of lymphocytes and macrophages were also present within alveolar septae. Occasional, small and discontinuous foci of type II pneumocyte hyperplasia were associated with the foci of alveolitis. These were considered to be a response to CS-induced inflammation and not primary hyperplastic lesions and, therefore, were not included as part of the proliferative lesion assessment. The inflammatory changes were distributed throughout the parenchyma of all lung lobes and were present to some extent in nearly all CS-exposed mice examined. Minimal to mild peribronchiolar and perivascular lymphoid aggregates were present in the lungs of aging sham-exposed mice; however, these changes were not associated with the other inflammatory lesions identified in the lungs of CS-exposed mice.

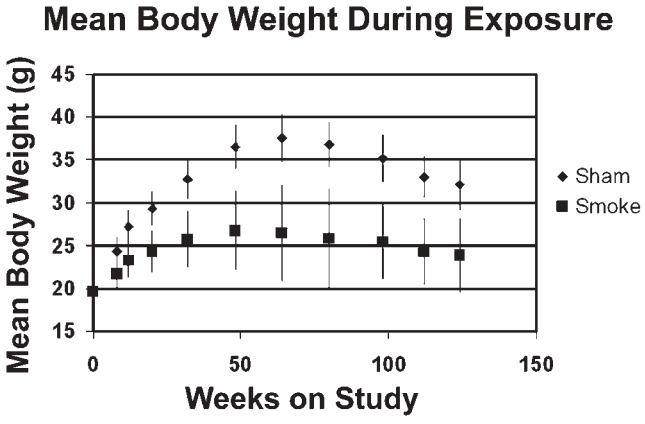

Fig. 2. Body weight of cigarette smoke-exposed and sham-exposed mice. Mean body weights of CS-exposed and sham-exposed mice throughout the exposure period are shown (mean ± standard deviation).

Incidence and multiplicity of hyperplastic and neoplastic lung lesions in CS-exposed and sham-exposed mice

The overall incidence of proliferative lung lesions in sham-exposed and CS-exposed mice is summarized in Table I. CS exposure resulted in a statistically significant increase in the incidence of all lung neoplasms and hyperplastic foci. The increase in the incidence of lung hyperplasia and neoplasia was first observed in CS-exposed mice that died spontaneously between 540 and 720 days after the initiation of exposure, with lesions present in 25% of CS-exposed mice and 7.2% of sham-exposed mice (data not shown).

Focal alveolar hyperplasia was characterized by discrete foci of proliferative type II pneumocytes forming a continuous lining along pre-existing alveolar septae (Figure 3A and B). The proliferating cells were typically present as a single layer, with neither the disruption of pulmonary architecture nor compression of adjacent structures. The hyperplastic type II cells exhibited minimal cytologic and nuclear atypia. Focal alveolar hyperplasias were detected in 17.9% (59/330) of CS-exposed mice compared with 1.8% (6/326) of sham-exposed mice ($P < 0.001$).

Bronchiolar epithelial hyperplasia was characterized by the proliferation of cuboidal/columnar cells of the conducting airways with frequent protrusions of small epithelial lined papillae into the airway lumina (data not shown). This change was widespread in the conducting airways of nearly all the CS-exposed mice, and was rarely present in the air exposed control mice.

Adenomas were characterized by solid, papillary or mixed growth patterns and consisted of well-circumscribed areas of proliferating polygonal to cuboidal/columnar cells with disruption of the pulmonary architecture and compression of adjacent parenchyma (Figure 3C and D). These cells sometimes exhibited cytoplasmic vacuolization and occasionally

Table I. Hyperplastic and neoplastic lung and nasal lesion incidence[a] in CS-exposed and sham-exposed mice

Lung lesion	Sham (%)	Smoke (%)	*P*-value[b]
Focal alveolar hyperplasia	6/326 (1.8)	59/330 (17.9)	$P < 0.001$
Adenoma	22/326 (6.7)	93/330 (28.2)	$P < 0.001$
Bronchiolar papilloma	0/326 (0)	15/330 (4.5)	$P < 0.007$
Total number of mice with benign neoplasms	22/326 (6.7)	102/330 (30.9)[c]	$P < 0.001$
Adenocarcinoma	9/326 (2.8)	67/330 (20.3)	$P < 0.001$
Total number of mice with all lung neoplasms	31/326 (9.5)	148/330 (44.8)[c]	$P < 0.001$
Total with distant metastases of lung neoplasm	1/326 (0.31)	5/330 (1.52)	$P < 0.001$
Nasal lesion			
Squamous cell carcinoma	0/326 (0)	9/330 (2.7)	Not determined
Squamous cell carcinoma-*in-situ*	0/326 (0)	5/330 (1.5)	Not determined
Hemangioma	0/326 (0)	5/330 (1.5)	Not determined
Respiratory papilloma	0/326 (0)	1/330 (0.3)	Not determined
Total number of mice with all nasal cavity neoplasms	0/326 (0)	20/330 (6.1)	$P < 0.001$

[a]Incidence is defined as the number of mice having at least one of the designated lesions per total mice in the exposure group.
[b]Logistic regression test.
[c]These totals are less than the sum of the neoplasms enumerated in the rows above because many mice had multiple lung neoplasms.

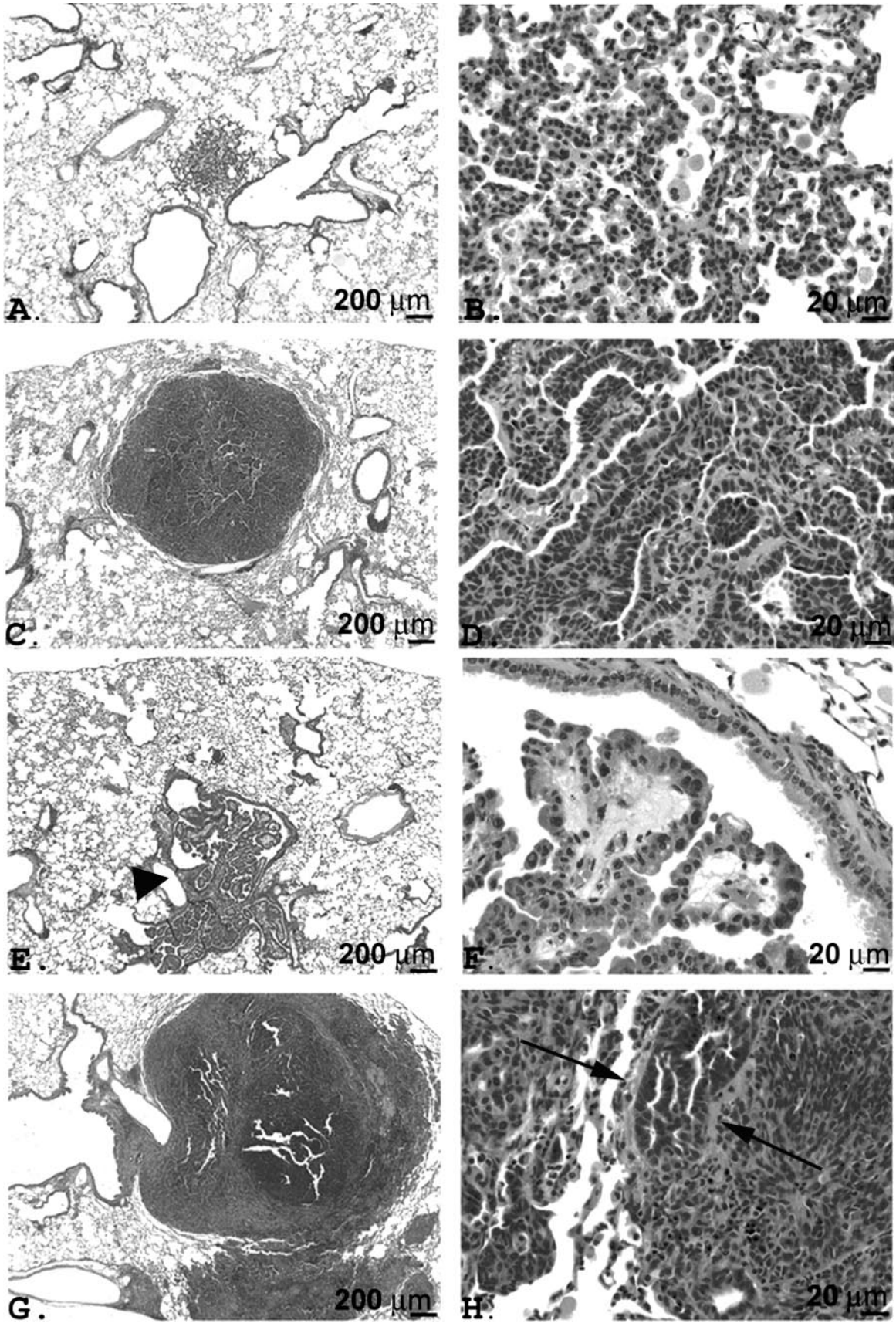

Fig. 3. Proliferative lesions in the CS-exposed B6C3F1 mouse lung. (**A**) and (**B**) Low and high power views of focal alveolar hyperplasia; (**C**) and (**D**) low and high power views of papillary adenoma; (**E**) and (**F**) low and high power views of bronchiolar papilloma (arrowhead denotes fibrovascular stalk; (**G**) and (**H**) low and high power views of papillary adenocarcinoma. Neoplastic cells fill a vessel lumen (demarcated by arrows). H&E stain.

appeared to produce mucus. In solid adenomas, the proliferating cells lined and filled the alveoli. In papillary adenomas, proliferating cells lined thin fibrovascular projections into the alveoli. The mixed adenomas consisted of a mixture of the two subtypes. Foci with hyperchromasia and cytologic and/or nuclear atypia were observed in some adenomas, and either of these alone was not taken to be indicative of malignancy. Adenomas were detected in 28.2% (93/330) of CS-exposed mice compared with 6.7% (22/326) of sham-exposed mice ($P < 0.001$).

Papillomas were characterized by the presence of complex papillary structures formed by fibrovascular cores lined with proliferating cuboidal/columnar cells, which projected into the lumen of bronchioles (Figure 3E and F). These tumors often appeared to have arisen from the conducting airway epithelium. Epithelial cells comprising these tumors typically were well-differentiated and growth occurred by expansion through the airway lumen rather than invasion. Papillomas were detected in 4.5% (15/330) of CS-exposed mice and were not detected in any of the sham-exposed mice ($P < 0.001$).

Adenocarcinomas consisted of solid, papillary and mixed subtypes. Adenocarcinomas usually effaced the pulmonary architecture and had a greater degree of cytologic and nuclear atypia, a higher mitotic rate, a larger size and more regional variations in growth patterns than adenomas (Figure 3G and H). Invasion of neoplastic cells into airways, vessels, lymphatics and the pleural surfaces typified many adenocarcinomas, and local invasion to the surface of the heart, aorta and other thoracic structures was not uncommon. Adenocarcinomas were detected in 20.3% (67/330) of CS-exposed mice compared with 2.8% (9/326) of sham-exposed mice ($P < 0.001$). Of the 67 adenocarcinomas detected in CS-exposed mice, 25 were between 6 and 10 mm in diameter and 16 were >1 cm in diameter. Of the nine adenocarcinomas detected in sham-exposed mice, five were between 6 and 10 mm in diameter and none were >1 cm in diameter. Intrapulmonary metastases to the lung lobe of origin and to other lung lobes, as determined by the size, distribution and histological appearance of the metastases compared with the primary tumor, occurred in 25–30% of the adenocarcinomas from both CS- and sham-exposed mice. Although not a statistically significant difference, extra-pulmonary metastases were detected in a higher number of CS-exposed mice (5/330 or 1.52%) compared with sham-exposed mice (1/326 or 0.31%). Only grossly identifiable metastatic lesions were included in this enumeration. The most common site of extra-thoracic metastases was the kidney.

CS exposure also resulted in a significant increase in the multiplicity of primary proliferative lung lesions in the mice in this study (Table II). Most sham-exposed mice bearing a proliferative primary lung lesion had only one lesion. In contrast, 167 CS-exposed mice had 282 proliferative primary lung lesions (68 hyperplastic foci and 214 tumors) with an average of 1.69 lesions per mouse having a lesion.

Other lung neoplasms

Other neoplastic lesions identified in the lungs included lymphosarcoma, metastatic hepatocellular carcinoma, metastatic mammary carcinoma, metastatic histiocytic sarcoma and metastatic osteosarcoma. Lymphosarcoma occurred at a reduced rate and exhibited a later onset in CS-exposed mice (7.6% incidence, 676 days first case) compared with sham-exposed mice (27.0% incidence, 322 days first case) ($P < 0.001$).

Table II. Hyperplastic and neoplastic lung lesion multiplicity[a] in CS-exposed and sham-exposed mice

Lesion	Sham (average number/mouse ± standard error)	Smoke (average number/mouse ± standard error)
Focal alveolar hyperplasia	1.17 ± 0.44 (7/6)	1.15 ± 0.44 (68/59)
Tumors (benign plus malignant)	1.03 ± 0.03 (32/31)	1.45 ± 0.06 (214/148)[b]
All proliferative (hyperplasias plus tumors)	1.08 ± 0.05 (39/36)	1.69 ± 0.07 (282/167)[c]

[a]Multiplicity is defined as the total number of the lesions observed divided by the number of mice bearing at least one of the designated lesions.
[b]$P < 0.001$.
[c]$P < 0.001$.

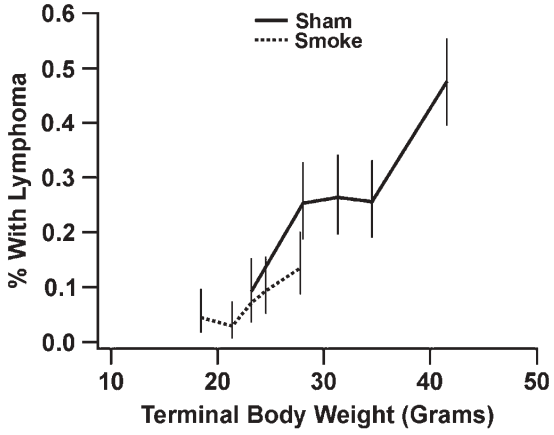

Fig. 4. Lymphoma incidence versus body weight. Mean values of weight quintiles are on the *x*-axis. Error bars reflect 95% binomial confidence limits. The relationship between body weight and lymphosarcoma incidence is the same for CS- and sham-exposed mice.

The incidence of lymphosarcoma was weight-related in both CS-exposed ($P = 0.003$) and sham-exposed ($P < 0.001$) mice, and the relationship between lymphosarcoma incidence and body weight was not significantly different between the exposure groups (Figure 4). Thus, it was concluded that the reduced incidence of lymphosarcoma in CS-exposed mice was due to their lower body weight. A reduction in the incidence and delay in onset of other metastatic tumors (primarily hepatocellular carcinoma) identified in the lungs were also evident in CS-exposed mice (5.8% incidence, 444 days first case) compared with sham-exposed mice (12.0% incidence, 375 days first case) ($P = 0.03$). These results are consistent with previous reports demonstrating a repressive influence of reduced body weight on the incidence of lymphosarcoma and other neoplasia in B6C3F1 mice (47,49).

Nasal lesions

Non-neoplastic lesions within the nasal cavity were present to some degree in nearly all CS-exposed mice and included neutrophilic rhinitis and sinusitis, respiratory epithelial hyperplasia with foci of squamous metaplasia, and foci of olfactory epithelial atrophy and respiratory epithelial metaplasia of the olfactory epithelium. Lesions in the olfactory epithelial regions were often accompanied by atrophy of the submucosal olfactory nerves and turbinates. Olfactory epithelial atrophy was observed to a slight degree in a few control mice and was interpreted to represent an age-related change.

Nasal cavity neoplasms were only observed in the CS-exposed mice ($P < 0.001$) (Table I). Of the 330 CS-exposed mice, 20 exhibited nasal cavity neoplasms. Squamous cell carcinoma (Figure 5) was the most commonly observed neoplasm (9/20) followed by squamous cell carcinoma-*in-situ* (5/20), hemangioma (5/20) and respiratory papilloma (1/20).

K-ras mutations in lung tumors from CS- and sham-exposed mice

The results of the *K-ras* codon 12 mutation analysis are summarized in Table III, and an example of the restriction fragment polymorphism analysis for representative tumors is shown in Figure 6A. *K-ras* mutations were detected at codon 12 in 47% (7/15) and 60% (27/45) of the lung tumors from sham and CS-exposed mice, respectively. For those mice having codon 12 mutations, the rates of transversion mutations and transition mutations were similar between the sham- (57% transversions and 43% transitions) and CS- (63% transversions and 37% transitions) exposed groups. However, malignant tumors from CS-exposed mice exhibited a greater mutation spectrum at codon 12, with detection of CGT and AGT mutations in addition to the more commonly observed GTT and GAT mutations. Comparison of the percentage of tumors with transition mutations, transversion mutations or no mutations at codon 12 demonstrated no significant differences ($P > 0.05$, Fisher's exact test) between the two exposure groups.

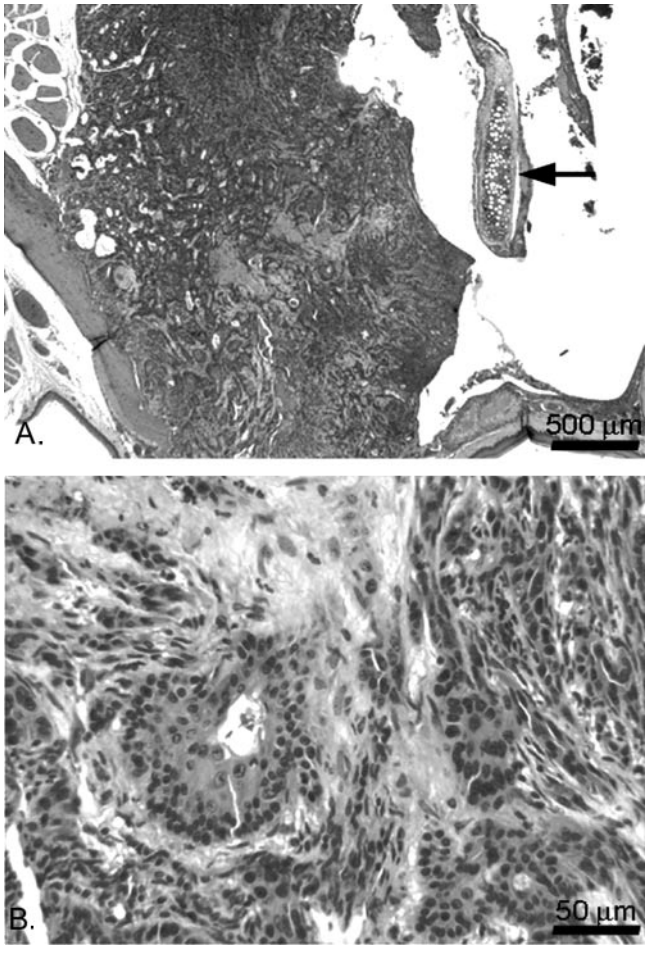

Fig. 5. Squamous cell carcinoma in the nasal cavity of a CS-exposed B6C3F1 mouse. Low (**A**) and high (**B**) power views. The arrow denotes the nasal septum. H&E stain.

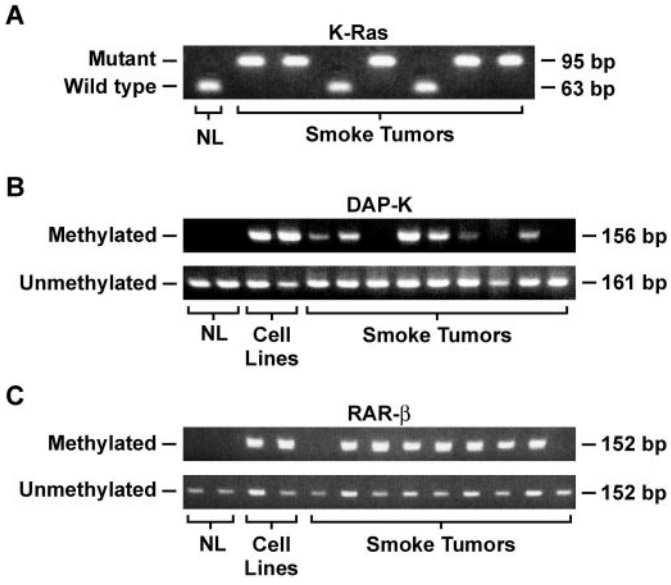

Fig. 6. Mutation and methylation analysis of murine lung tumors. (**A**) Restriction fragment length polymorphism analysis of *K-ras* codon 12 mutations. Second stage PCR reaction products are digested with BstN1. The restriction fragment generated from normal mouse lung in the absence of codon 12 mutations is 63 bp (far left). Tumors from mice with mutations in codon 12 do not digest yielding a 95 bp fragment after the BstN1 digestion. (**B**) *DAP-kinase* methylation-specific PCR. Tumors with DAP-kinase methylation are indicated by the presence of a 156 bp methylation band. (**C**) *RAR*-β methylation-specific PCR. Tumors with *RAR*-β methylation are indicated by a 152 bp methylation band. Normal lung (NL) from B6C3F1 mice serve as negative control tissue. The cell lines from NNK-induced murine lung tumors serve as positive controls. The appearance of unmethylated bands in the tumors and cell lines that also exhibit methylated bands is due to the presence of unmethylated alleles (tumors and cell lines) and/or contaminating adjacent normal tissues (tumors).

Table III. Codon 12 *k-ras* mutations in lung tumors from CS- and sham-exposed mice

	No. of tumors examined	GGT→GTT (%)	GGT→GAT (%)	GGT→CGT (%)	GGT→AGT (%)	Transitions (%)	Transversions (%)
Smoke							
Benign	13	3/13 (23)	2/13 (15)	0/13 (0)	0/13 (0)	2/13 (15)	3/13 (23)
Malignant	32	11/32 (34)	7/32 (22)	3/32 (9)	1/32 (4)	8/32 (25)	14/32 (44)
All tumors	45	14/45 (31)	9/45 (20)	3/45 (6.7)	1/45 (2.2)	10/45 (22)	17/45 (38)
Sham							
Benign	8	2/8 (25)	3/8 (38)	0/8 (0)	0/8 (0)	3/8 (38)	2/8 (25)
Malignant	7	2/7 (29)	0/7 (0)	0/7 (0)	0/7 (0)	0/7	2/7 (29)
All tumors	15[a]	4/15 (27)	3/15 (20)	0/15 (0)	0/15 (0)	3/15 (20)	4/15 (27)

[a]Because of insufficient amounts of sample, only 14/15 of these tumors from sham-exposed mice were also analyzed for promoter methylation.

Table IV. *RAR*-β and *DAP-kinase* hypermethylation in lung tumors from CS-exposed and sham-exposed mice

	No. of tumors examined	RAR-β methylated (%)	*DAP-kinase* methylated (%)	Either *RAR*-β or DAP-kinase methylation (%)
Smoke[a]				
Benign	11/37 (30)	8/11 (73)	7/11 (64)	10/11 (91)
Malignant	26/37 (70)	23/26 (88)	16/26 (62)	24/26 (92)
All tumors	37[b]	31/37 (84)	23/37 (62)	34/37 (92)[c]
Sham				
Benign	7/15 (53)	3/7 (43)	3/7 (43)	3/7 (43)
Malignant	8/15 (47)	6/8 (75)	3/8 (38)	6/8 (75)
All tumors	15[d]	9/15 (60)	6/15 (40)	10/15 (67)

[a]Methylation results for 14 of these tumors were previously reported (14,15).
[b]Because of insufficient amounts of sample, only 37 of the 45 tumors that were analyzed for *K-ras* mutations were also analyzed for methylation of *RAR*-β and *DAP-kinase*.
[c]$P = 0.036$, Fisher's exact test.
[d]Because of insufficient amounts of sample, only 14/15 tumors from sham-exposed mice were also analyzed for *K-ras* mutations.

DAP-kinase and RAR-β methylation in lung tumors from CS- and sham-exposed mice

The results of the promoter methylation analysis for *DAP-kinase* and *RAR*-β are summarized in Table IV, and are shown in Figure 6B and C for representative tumor samples. Methylation of the *DAP-kinase* and *RAR*-β promoters in murine lung tumors detected by the MSP assay is associated with transcriptional silencing of these genes (14,15). *DAP-kinase* and *RAR*-β were hypermethylated in 62 and 84% of lung tumors from the CS-exposed mice, respectively. In sham-exposed control mice, *DAP-kinase* and *RAR*-β were hypermethylated in 40 and 60% of the lung tumors examined, respectively. There was a positive association between CS exposure and methylation of either *DAP-kinase* or *RAR*-β or both ($P = 0.036$), and a trend towards an association between CS exposure and *RAR*-β methylation ($P = 0.081$). Methylation of *DAP-kinase* and *RAR*-β was independent of the codon 12 *K-ras* mutation status ($P > 0.05$). The methylation incidence for these genes also did not differ significantly between benign and malignant tumors.

Discussion

The results of this study show for the first time that near life time whole body exposures to mainstream CS induces marked, exposure-related increases in the incidence and multiplicity of hyperplastic, benign and malignant epithelial lesions in the lungs of female B6C3F1 mice. These results are noteworthy because of the statistical strength of the association between proliferative pulmonary lesions and CS exposure, particularly for a mouse strain that has a low baseline incidence of pulmonary neoplasia. Furthermore, the standard lung sections examined likely overlooked small tumors that would have been detected if serial sections had been examined. Because the CS exposure group had more lung tumors, the undercounting of tumors likely had a greater effect on the lung tumor incidence in the CS-exposed animals compared with the sham-exposed animals. The presence of activating point mutations in the *K-ras* gene and epigenetic silencing of the *DAP-kinase* and *RAR*-β genes in murine lung tumors as well as human adenocarcinomas confirms the importance of these genes in lung tumorigenesis and attests to the relevance of this mouse model.

The reason for the marked induction of lung tumors in the mice in this study compared with previous studies is uncertain, but is likely related to the long duration of exposure (918 days) and the increased lung doses provided by protracted, daily whole body exposures. This finding is similar to that observed in humans, where the risk for lung cancer increases with age and the duration of smoking (50). A previous report estimated that exposure of rats to this concentration of total particulate matter from CS is equivalent to a human smoking 3–4 packs of cigarettes a day (51). In addition, transdermal and gastrointestinal (after grooming) exposures to CS-derived carcinogens is likely, and this may also have played a role in lung carcinogenesis. This study also demonstrates a statistically significant CS exposure-related increase in the incidence of benign and malignant proliferative lesions in the nasal cavity. These results confirm those of a recent study in which a weaker, but statistically significant induction of lung and nasal cavity tumors in F344 rats was demonstrated (9).

In spite of the higher lung tumor incidence and multiplicity in CS-exposed mice, survival of these mice was significantly longer than for the sham-exposed mice. Longer survival in the CS-exposed mice is likely a sequela of the lower incidence and delayed onset of other types of fatal neoplasia, in part due to the reduced body weight in these mice. The reason for the lower body weight in CS-exposed mice is not certain; however, a previous study in rats showed a dose-related depression in food consumption, which began as early as 2 weeks after the start of CS exposures and continued even after 61 weeks of CS exposure (9). This is similar to the situation in human smokers, who tend to have lower body weight than nonsmokers and who tend to gain weight after the cessation of smoking. In B6C3F1 mice, food restriction and lower body weight has a significant repressive influence on the incidence of many tumor types, including hepatocellular carcinoma and lymphosarcoma (47,49). A comparison of terminal body weight with lymphosarcoma incidence for mice in this study showed that lymphosarcoma incidence is weight-related for both the CS-exposed ($P = 0.003$) and sham-exposed animals ($P < 0.001$) and, furthermore, that the relationship between the incidence of lymphosarcoma and body weight is the same for both the groups (Figure 4). These observations support the hypothesis that the decreased body weight in CS-exposed mice results in decreased lymphosarcoma and hepatic carcinoma incidences, which contributes to their increased survival. To accurately evaluate the effect of CS on survival without the confounding influence of body weight, sham-exposed animals could be food restricted in future studies.

While decreased weight gain in CS-exposed B6C3F1 mice likely enhances their survival, increased survival is unlikely to have increased the incidence of lung tumor formation in these mice. In fact, food restriction and lower body weight typically represses development of multiple tumor types in mice. Sheldon *et al*. (49) demonstrated that food restricted B6C3F1 mice, offered 60% of the diet consumed by *ad libitum* fed B6C3F1 mice, had a 36% increase in median survival age in both the sexes and a 22–33% increase in maximal lifespan compared with those that were fed *ad libitum*. The food restricted female mice maintained a relatively constant body weight, between 22 and 24 g from 6.25 months of age until the end of the study, whereas the *ad libitum* fed females gained weight until a maximum of 38.5 g at 2 years of age, then declined. The increased lifespan in these animals was shown to be due to a decrease in the incidence of fatal tumors, most prominently

lymphosarcoma. Importantly, despite their extended lifespan and subsequent increased opportunity for lung tumor development, the food restricted female mice had a similar incidence of lung tumor formation (10.6%) as the *ad libitum* fed female mice (8.1%). These results suggest that the increased lifespan of the CS-exposed mice in our study did not contribute to the observed increased lung tumor incidence and multiplicity. The tumor repressive effect of lower body weight in mice may also explain why previous, shorter duration studies of CS-induced lung cancer in A/J mice required a 4 month recovery period in air in order to show an increase in lung tumor formation compared with controls (4–6). During the 4 month recovery period, the CS-exposed mice gained weight to match the weight of the control mice, which may have removed the inhibitory effect of reduced caloric consumption and lower body weight on lung tumor development.

Comparison of the CS-induced lung lesions in B6C3F1 mice with those of chronic human smokers reveals many similarities. The chronic inflammatory lesions, characterized by the accumulation of pigment-laden alveolar macrophages and neutrophils, and peribronchiolar and perivascular lymphocytes are similar to the inflammatory changes described in humans after chronic CS exposures (52,53). Although not evaluated in this study, a previous report demonstrated that this exposure regime also induces emphysema in B6C3F1 mice and rats (54). The neoplastic lung lesions in the mice in this study were primarily adenomas and adenocarcinomas that originated in the peripheral lung. These tumors originate from alveolar type II cells, and are preceded by hyperplastic foci (26). Lung cancer in humans is represented by a more diverse morphologic spectrum than what occurs in the mouse, which may be a reflection of the more complex epithelium of the human conducting airways compared with those of the mouse. Adenocarcinoma is, nevertheless, the most common type of human lung cancer and many cases of human lung adenocarcinoma also originate from the peripheral lung from pre-existing atypical hyperplastic foci (55,56).

The frequency of codon 12 *K-ras* mutations in mouse lung tumors (47–60%) is comparable to what has been described in human lung tumors (22–56%) (17–22), and the proportion of transversion and transition mutations observed in murine lung tumors was similar to that reported for human lung tumors. In some reports, lung tumors from human smokers have a higher codon 12 *K-ras* mutation frequency than those from non-smokers (18,19). However, other reports demonstrate a similar codon 12 *K-ras* mutation frequency and profile for human smokers (24%) and non-smokers (22%) (20). The variation in the results reported for human non-smokers may be due to differences in the sensitivity of the detection assays used or confounding effects of exposure to environmental tobacco smoke in human non-smokers. In this study, lung tumors from CS-exposed mice exhibit a similar codon 12 mutation frequency and profile compared with tumors derived from sham-exposed mice. However, the malignant tumors from CS-exposed mice do exhibit a greater mutation spectrum at codon 12, with detection of CGT and AGT mutations in addition to the more commonly observed GTT and GAT mutations. Witschi *et al*. evaluated *K-ras* mutations in tumors from CS-exposed and sham-exposed A/J mice and reported that none of the mice exhibited mutations at codon 12, and the mutation frequency at codon 61 was similar for both the groups (5). The relative lack of specificity of *K-ras* mutations in tumors from CS-exposed mice and humans likely reflects the complex mixture of carcinogenic substances present in CS.

Hypermethylation of *DAP-kinase* occurs in lung tumors evaluated from sham-exposed mice (40%) and CS-exposed mice (62%). These methylation frequencies are similar to those reported for mouse lung tumors induced by methylene chloride (50%), vinyl carbamate (60%) and NNK (52%), and for NNK-induced hyperplastic foci (46%) (15). The transcriptional silencing of *DAP-kinase* in hyperplastic lesions suggests that *DAP-kinase* methylation is an early event in lung tumorigenesis. *DAP-kinase* hypermethylation has also been reported in human lung adenocarcinomas at a similar rate for smokers and never-smokers (36%) (57).

While the difference between *RAR*-β hypermethylation in lung tumors from CS-exposed mice (84%) and sham-exposed mice (60%) was not statistically significant, there was a tendency ($P = 0.081$) for increased prevalence of *RAR*-β methylation in tumors from CS-exposed mice. The lack of statistical significance is, at least in part, due to the small number of samples available for evaluation. When data from the entire pool of previously analyzed CS-induced murine lung tumors (14) are included in the statistical evaluation (data not shown), a statistically significant relationship between CS exposure and *RAR*-β methylation is evident ($P < 0.05$). *RAR*-β hypermethylation has also been reported in 85% of NNK-induced lung tumors, but only in 56 and 60% of lung tumors induced by methylene chloride and vinyl carbamate, respectively (14). The similar methylation frequencies in tumors from CS-exposed mice and NNK-exposed mice suggest that NNK may be the dominant carcinogen in CS responsible for *RAR*-β silencing. *RAR*-β is hypermethylated in 54% of NNK-induced hyperplasias in mice indicating that *RAR*-β has an early role in lung carcinogenesis and may also have a role in tumor progression. Previous results demonstrated methylation of DAP-kinase (one out of three) and RAR-β (two out of three) in the three cell lines derived from CS-induced murine lung tumors (14,15). In human lung cancer, *RAR*-β hypermethylation has been reported in 41% of human non-small cell lung cancers (33).

These studies emphasize the importance of *DAP-kinase* and *RAR*-β hypermethylation in both spontaneous and carcinogen-induced human and murine lung cancers. The detection of *DAP-kinase* and *RAR*-β methylation in spontaneous tumors reinforces the premise that epigenetic silencing in cancer is not a random process but is targeted to abrogating critical pathways needed for cellular homeostasis. Currently, the mechanisms leading to targeting of specific genes for silencing through promoter hypermethylation are unknown.

The goal of this investigation was to develop a murine model of CS-induced lung cancer for a subsequent characterization of the molecular mechanisms involved in neoplastic transformation of the lung. The identification of genetic and epigenetic changes in three genes in these mice that are similar to those identified in human lung cancer suggest that this model will be useful for discovering new pathways that contribute to the initiation and promotion of human lung cancer. As new signaling pathways are identified, additional molecular markers for early detection and new molecular targets for prevention and therapy of lung cancer may be identified. This model may also be useful for testing putatively safer tobacco formulations or cigarette designs, for evaluating the efficacy of chemopreventative or therapeutic agents, and for defining the interactions between cigarette smoking and other carcinogens in the development of lung cancer.

Acknowledgements

The authors would like to thank the members of the Institute's staff who made scientific, technical and administrative contributions to the research. This work was supported by National Institutes of Health Grant RR00136CA, National Institute of Environmental Health Sciences Grant ES08801, and by the Offices of Defense Programs and Health and Environmental Research, U.S. Department of Energy, under Cooperative Agreement No. DE-FC04-96AL76406. The research was conducted in facilities fully accredited by the Association for the Assessment and Accreditation of Laboratory Animal Care International.

Conflict of Interest Statement: Dr Belinsky is a consultant to Oncomethylome Sciences, Inc. Under a licensing agreement between Lovelace Respiratory Research Institute and Oncomethylome Sciences, nested methylation-specific PCR was licensed to Oncomethylome Sciences, and the author is entitled to a share of the royalties received by the institute from the sales of this licensed technology. The institute, in accordance with its conflict of interest policies, is managing the terms of these arrangements.

References

1. American Cancer Society. Cancer Facts and Figures. (2003) *Surveillance Research*. American Cancer Society, Atlanta, Georgia, pp. 13–14.
2. Thun,M.J., Lally,C.A., Flannery,J.T., Calle,E.E., Flanders,W.D. and Heath,C.W.Jr. (1997) Cigarette smoking and changes in the histopathology of lung cancer. *J. Natl Cancer Inst*., **89**, 1580–1586.
3. Wingo,P.A., Ries,L.A., Giovino,G.A., Miller,D.S., Rosenberg,H.M., Shopland,D.R., Thun,M.J. and Edwards,B.K. (1999) Annual report to the nation on the status of cancer, 1973–1996, with a special section on lung cancer and tobacco smoking. *J. Natl Cancer Inst*., **91**, 675–690.
4. Curtin,G.M., Higuchi,M.A., Ayres,P.H., Swauger,J.E. and Mosberg,A.T. (2004) Lung tumorigenicity in A/J and rasH2 transgenic mice following mainstream tobacco smoke inhalation. *Toxicol. Sci*., **81**, 26–34.
5. Witschi,H., Espiritu,I., Dance,S.T. and Miller,M.S. (2002) A mouse lung tumor model of tobacco smoke carcinogenesis. *Toxicol. Sci*., **68**, 322–330.
6. Witschi,H., Espiritu,I., Peake,J.L., Wu,K., Maronpot,R.R. and Pinkerton,K.E. (1997) The carcinogenicity of environmental tobacco smoke. *Carcinogenesis*, **18**, 575–586.
7. D'Agostini,F., Balansky,R.M., Bennicelli,C., Lubet,R.A., Kelloff,G.J. and De Flora,S. (2001) Pilot studies evaluating the lung tumor yield in cigarette smoke-exposed mice. *Int. J. Oncol*., **18**, 607–615.
8. Finch,G.L., Nikula,K.J., Belinsky,S.A., Barr,E.B., Stoner,G.D. and Lechner,J.F. (1996) Failure of cigarette smoke to induce or promote lung cancer in the A/J mouse. *Cancer Lett*., **99**, 161–167.
9. Mauderly,J.L., Gigliotti,A.P., Barr,E.B., Bechtold,W.E., Belinsky,S.A., Hahn,F.F., Hobbs,C.A., March,T.H., Seilkop,S.K. and Finch,G.L. (2004) Chronic inhalation exposure to mainstream cigarette smoke increases lung and nasal tumor incidence in rats. *Toxicol. Sci*., **85**, 447–459.
10. Coggins,C.R. (2002) A minireview of chronic animal inhalation studies with mainstream cigarette smoke. *Inhal. Toxicol*., **14**, 991–1002.
11. Coggins,C.R. (2001) A review of chronic inhalation studies with mainstream cigarette smoke, in hamsters, dogs, and nonhuman primates. *Toxicol. Pathol*., **29**, 550–557.
12. Coggins,C.R. (1998) A review of chronic inhalation studies with mainstream cigarette smoke in rats and mice. *Toxicol. Pathol*., **26**, 307–314; discussion 315.
13. Belinsky,S.A., Swafford,D.S., Middleton,S.K., Kennedy,C.H. and Tesfaigzi,J. (1997) Deletion and differential expression of p16INK4a in mouse lung tumors. *Carcinogenesis*, **18**, 115–120.
14. Vuillemenot,B.R., Pulling,L.C., Palmisano,W.A., Hutt,J.A. and Belinsky,S.A. (2004) Carcinogen exposure differentially modulates *RAR-beta* promoter hypermethylation, an early and frequent event in mouse lung carcinogenesis. *Carcinogenesis*, **25**, 623–629.
15. Pulling,L.C., Vuillemenot,B.R., Hutt,J.A., Devereux,T.R. and Belinsky,S.A. (2004) Aberrant promoter hypermethylation of the death-associated protein kinase gene is early and frequent in murine lung tumors induced by cigarette smoke and tobacco carcinogens. *Cancer Res*., **64**, 3844–3848.
16. Bonner,A.E., Lemon,W.J., Devereux,T.R., Lubet,R.A. and You,M. (2004) Molecular profiling of mouse lung tumors: association with tumor progression, lung development, and human lung adenocarcinomas. *Oncogene*, **23**, 1166–1176.
17. Mills,N.E., Fishman,C.L., Rom,W.N., Dubin,N. and Jacobson,D.R. (1995) Increased prevalence of *K-ras* oncogene mutations in lung adenocarcinoma. *Cancer Res*., **55**, 1444–1447.
18. Ahrendt,S.A., Decker,P.A., Alawi,E.A., Zhu Yr,Y.R., Sanchez-Cespedes,M., Yang,S.C., Haasler,G.B., Kajdacsy-Balla,A., Demeure,M.J. and Sidransky,D. (2001) Cigarette smoking is strongly associated with mutation of the *K-ras* gene in patients with primary adenocarcinoma of the lung. *Cancer*, **92**, 1525–1530.
19. Marchetti,A., Pellegrini,S., Sozzi,G., Bertacca,G., Gaeta,P., Buttitta,F., Carnicelli,V., Griseri,P., Chella,A., Angeletti,C.A., Pierotti,M. and Bevilacqua,G. (1998) Genetic analysis of lung tumours of non-smoking subjects: *p53* gene mutations are constantly associated with loss of heterozygosity at the FHIT locus. *Br. J. Cancer*, **78**, 73–78.
20. Pulling,L.C., Divine,K.K., Klinge,D.M., Gilliland,F.D., Kang,T., Schwartz,A.G., Bocklage,T.J. and Belinsky,S.A. (2003) Promoter hypermethylation of the *O*6-methylguanine-DNA methyltransferase gene: more common in lung adenocarcinomas from never-smokers than smokers and associated with tumor progression. *Cancer Res*., **63**, 4842–4848.
21. Keohavong,P., Mady,H.H., Gao,W.M., Siegfried,J.M., Luketich,J.D. and Melhem,M.F. (2001) Topographic analysis of *K-ras* mutations in histologically normal lung tissues and tumours of lung cancer patients. *Br. J. Cancer*, **85**, 235–241.
22. Nelson,H.H., Christiani,D.C., Mark,E.J., Wiencke,J.K., Wain,J.C. and Kelsey,K.T. (1999) Implications and prognostic value of *K-ras* mutation for early-stage lung cancer in women. *J. Natl Cancer Inst*., **91**, 2032–2038.
23. Ton,T.V., Hong,H.H., Anna,C.H., Dunnick,J.K., Devereux,T.R., Sills,R.C. and Kim,Y. (2004) Predominant *K-ras* codon 12 G→A transition in chemically induced lung neoplasms in B6C3F1 mice. *Toxicol. Pathol*., **32**, 16–21.
24. Hecht,S.S. (1999) DNA adduct formation from tobacco-specific N-nitrosamines. *Mutat. Res*., **424**, 127–142.
25. Belinsky,S.A., Devereux,T.R., Maronpot,R.R., Stoner,G.D. and Anderson,M.W. (1989) Relationship between the formation of promutagenic adducts and the activation of the *K-ras* protooncogene in lung tumors from A/J mice treated with nitrosamines. *Cancer Res*., **49**, 5305–5311.
26. Belinsky,S.A., Devereux,T.R., Foley,J.F., Maronpot,R.R. and Anderson,M.W. (1992) Role of the alveolar type II cell in the development and progression of pulmonary tumors induced by 4-(methylnitrosamino)-1-(3-pyridyl)-1-butanone in the A/J mouse. *Cancer Res*., **52**, 3164–3173.
27. Herman,J.G. and Baylin,S.B. (2003) Gene silencing in cancer in association with promoter hypermethylation. *N. Engl. J. Med*., **349**, 2042–2054.
28. Esteller,M., Sanchez-Cespedes,M., Rosell,R., Sidransky,D., Baylin,S.B. and Herman,J.G. (1999) Detection of aberrant promoter hypermethylation of tumor suppressor genes in serum DNA from non-small cell lung cancer patients. *Cancer Res*., **59**, 67–70.
29. Kim,D.H., Nelson,H.H., Wiencke,J.K., Christiani,D.C., Wain,J.C., Mark,E.J. and Kelsey,K.T. (2001) Promoter methylation of DAP-kinase: association with advanced stage in non-small cell lung cancer. *Oncogene*, **20**, 1765–1770.
30. Tang,X., Khuri,F.R., Lee,J.J., Kemp,B.L., Liu,D., Hong,W.K. and Mao,L. (2000) Hypermethylation of the death-associated protein (DAP)-kinase promoter and aggressiveness in stage I non-small-cell lung cancer. *J. Natl Cancer Inst*., **92**, 1511–1516.
31. Raffo,P., Emionite,L., Colucci,L., Belmondo,F., Moro,M.G., Bollag,W. and Toma,S. (2000) Retinoid receptors: pathways of proliferation inhibition and apoptosis induction in breast cancer cell lines. *Anticancer Res*., **20**, 1535–1543.
32. Treutin,P.M., Chen,L.I., Buetow,B.S., Zeng,W., Birkebak,T.A., Seewaldt,V.L., Sommer,K.M., Emond,M., Maggio-Price,L. and Swisshelm,K. (2002) Retinoic acid receptor beta2 inhibition of metastasis in mouse mammary gland xenografts. *Breast Cancer Res. Treat*., **72**, 79–88.
33. Virmani,A.K., Rathi,A., Zochbauer-Muller,S., Sacchi,N., Fukuyama,Y., Bryant,D., Maitra,A., Heda,S., Fong,K.M., Thunnissen,F., Minna,J.D. and Gazdar,A.F. (2000) Promoter methylation and silencing of the retinoic acid receptor-beta gene in lung carcinomas. *J. Natl Cancer Inst*., **92**, 1303–1307.
34. Chen,B.T., Namenyi,J., Yeh,H.C., Mauderly,J.L. and Cuddihy,R.G. (1990) Physical characterization of cigarette smoke aerosol generated from a Walton smoke machine. *Aerosol. Sci. Technol*., **12**, 364–375.
35. Chen,B.T., Bechtold,W.E., Barr,E.B., Cheng,Y.S., Mauderly,J.L. and Cuddihy,R.G. (1989) Comparison of cigarette smoke exposure atmospheres in different exposure and puffing modes. *Inhal. Toxicol*., **1**, 331–347.
36. Chen,B.T., Bechtold,W.E. and Mauderly,J.L. (1992) Description and evaluation of a cigarette smoke generation system for inhalation studies. *J. Aerosol Med*., **5**, 19–30.

37. Nikitin,A.Y., Alcaraz,A., Anver,M.R. *et al*. (2004) Classification of proliferative pulmonary lesions of the mouse: recommendations of the mouse models of human cancers consortium. *Cancer Res*., **64**, 2307–2316.
38. Jones-Bolin,S.E., Johansson,E., Palmisano,W.A., Anderson,M.W., Wiest,J.S. and Belinsky,S.A. (1998) Effect of promoter and intron 2 polymorphisms on murine lung *K-ras* gene expression. *Carcinogenesis*, **19**, 1503–1508.
39. Levi,S., Urbano-Ispizua,A., Gill,R., Thomas,D.M., Gilbertson,J., Foster,C. and Marshall,C.J. (1991) Multiple *K-ras* codon 12 mutations in cholangiocarcinomas demonstrated with a sensitive polymerase chain reaction technique. *Cancer Res*., **51**, 3497–3502.
40. Kaplan,E.L. and Meier,P. (1958) Nonparametric estimation for incomplete observations. *J. Am. Stat. Assoc*., **53**, 457–458.
41. Cox,D. (1972) Regression models and life tables. *J. R. Stat. Soc*., **1338**, 187–220.
42. Steel,R.G.D. and Torrie,J.H., (1980) *Principles and Procedures of Statistics*. McGraw-Hill Book Company, New York.
43. Dinse,G.E. and Lagakos,S.W. (1983) Regression analysis of tumour prevalence data. *J. R. Stat. Soc*., **32**, 236–248.
44. Dinse,G.E. and Haseman,J.K. (1986) Logistic regression analysis of incidental-tumor data from animal carcinogenicity experiments. *Fundam. Appl., Toxicol*., **6**, 44–52.
45. Peto,R., Pike,M.C., Day,N.E., Gray,R.G., Lee,P.N., Parish,S., Peto,J., Richards,S. and Wahrendorf,J. (1980) Guidelines for simple, sensitive significance tests for carcinogenic effects in long-term animal experiments. *IARC Monogr Eval Carcinog Risk Chem Hum Suppl*, pp. 311–426.
46. Grizzle,J.E., Starmer,C.F. and Koch,G.G. (1969) Analysis of categorical data by linear models. *Biometrics*, **25**, 489–504.
47. Seilkop,S.K. (1995) The effect of body weight on tumor incidence and carcinogenicity testing in B6C3F1 mice and F344 rats. *Fundam. Appl. Toxicol*., **24**, 247–259.
48. Hosmer,D.W.J. and Lemeshow,S. (1989) *Applied Logistic Regression*. John Wiley and Sons, New York.
49. Sheldon,W.G., Bucci,T.J., Hart,R.W. and Turturro,A. (1995) Age-related neoplasia in a lifetime study of *ad libitum*-fed and food-restricted B6C3F1 mice. *Toxicol. Pathol*., **23**, 458–476.
50. Peto,R., Darby,S., Deo,H., Silcocks,P., Whitley,E. and Doll,R. (2000) Smoking, smoking cessation, and lung cancer in the UK since 1950: combination of national statistics with two case-control studies. *Br. Med. J*., **321**, 323–329.
51. Finch,G.L., Lundgren,D.L., Barr,E.B., Chen,B.T., Griffith,W.C., Hobbs,C.H., Hoover,M.D., Nikula,K.J. and Mauderly,J.L. (1998) Chronic cigarette smoke exposure increases the pulmonary retention and radiation dose of 239Pu inhaled as 239PuO2 by F344 rats. *Health Phys*., **75**, 597–609.
52. Niewoehner,D.E., Kleinerman,J. and Rice,D.B. (1974) Pathologic changes in the peripheral airways of young cigarette smokers. *N. Engl. J. Med*., **291**, 755–758.
53. Fraig,M., Shreesha,U., Savici,D. and Katzenstein,A.L. (2002) Respiratory bronchiolitis: a clinicopathologic study in current smokers, ex-smokers, and never-smokers. *Am. J. Surg. Pathol*., **26**, 647–653.
54. March,T.H., Barr,E.B., Finch,G.L., Hahn,F.F., Hobbs,C.H., Menache,M.G. and Nikula,K.J. (1999) Cigarette smoke exposure produces more evidence of emphysema in B6C3F1 mice than in F344 rats. *Toxicol. Sci*., **51**, 289–299.
55. Westra,W.H. (2000) Early glandular neoplasia of the lung. *Respir. Res*., **1**, 163–169.
56. Westra,W.H., Baas,I.O., Hruban,R.H., Askin,F.B., Wilson,K., Offerhaus,G.J. and Slebos,R.J. (1996) *K-ras* oncogene activation in atypical alveolar hyperplasias of the human lung. *Cancer Res*., **56**, 2224–2228.
57. Divine,K.K., Pulling,L.C., Marron-Terada,P.G., Liechty,K.C., Kang,T., Schwartz,A.G., Bocklage,T.J., Coons,T.A., Gilliland,F.D. and Belinsky,S.A. (2005) Multiplicity of abnormal promoter methylation in lung adenocarcinomas from smokers and never smokers. *Int. J. Cancer*, **114**, 400–405.

Received February 18, 2005; revised June 3, 2005; accepted June 5, 2005